Molecular Crystals and Liquid Crystals

Publication details, including instructions for authors and subscription information:
http://www.tandfonline.com/loi/gmcl20

Phase Separation in the Organic Solid State: The Influence of Quenching Protocol in Unstable n-Alkane Blends

E. P. Gilbert [a] , A. Nelson [a] , D. Sutton [b] , N. Terrill [c] , C. Martin [d] , J. Lal [e] & E. Lang [e]

[a] Bragg Institute, Menai, New South Wales, Australia

[b] Bragg Institute, Menai, and CRC for Polymers, New South Wales, Australia

[c] DIAMOND Synchrotron, Rutherford Appleton Laboratory, Didcot, United Kingdom

[d] Synchrotron Radiation Source, Daresbury Laboratory, Warrington, United Kingdom

[e] Intense Pulsed Neutron Source, Argonne National Laboratory, Argonne, Illinois, United States

Version of record first published: 31 Aug 2006

To cite this article: E. P. Gilbert, A. Nelson, D. Sutton, N. Terrill, C. Martin, J. Lal & E. Lang (2005): Phase Separation in the Organic Solid State: The Influence of Quenching Protocol in Unstable n-Alkane Blends, Molecular Crystals and Liquid Crystals, 440:1, 93-105

To link to this article: http://dx.doi.org/10.1080/15421400590957882

Mol. Cryst. Liq. Cryst., Vol. 440, pp. 93–105, 2005

ISSN: 1542-1406 print/1563-5287 online
DOI: 10.1080/15421400590957882

Taylor & Francis
Taylor & Francis Group

Phase Separation in the Organic Solid State: The Influence of Quenching Protocol in Unstable *n*-Alkane Blends

E. P. Gilbert
A. Nelson
Bragg Institute, Menai, New South Wales, Australia

D. Sutton
Bragg Institute, Menai, and CRC for Polymers, New South Wales, Australia

N. Terrill
DIAMOND Synchrotron, Rutherford Appleton Laboratory, Didcot, United Kingdom

C. Martin
Synchrotron Radiation Source, Daresbury Laboratory, Warrington, United Kingdom

J. Lal
E. Lang
Intense Pulsed Neutron Source, Argonne National Laboratory, Argonne, Illinois, United States

Blends of normal alkanes form lamellar structures, when quenched from the melt, in which the separation of the individual chains may be controlled by the chain-length mismatch, molar composition, isotopic substitution and confinement. 2:1 $C_{28}H_{58}$:$C_{36}D_{74}$ mixtures have been investigated after subjection to a cooling rate varying over three orders of magnitude and intermediate annealing prior to reaching ambient. Quenching at 100°C/min yields similar behaviour to intermediate

Support by Access to Major Research Facilities is gratefully acknowledged. This work has benefited from the use of the Intense Pulsed Neutron Source at Argonne National Laboratory which is funded by the U.S. Department of Energy, BES-Materials Science, under Contract W-31-109-ENG-38. We would also like to thank the staff at the SRS and Professor Charles Han at the Institute of Chemistry, Chinese Academy of Sciences who first suggested this experiment.

Address correspondence to E. P. Gilbert, Bragg Institute, PMB 1, Menai, NSW 2234, Australia. E-mail: epg@ansto.gov.au

annealing between the pure components' melting points. Slow cooling at 0.1°C/min generates significantly greater ordering and behaviour comparable to that obtained from annealing mid-way between the mixing transition and the $C_{28}H_{58}$ melting point.

Keywords: DSC; lamellar structures; *n*-alkane blends; SANS; SAXS

INTRODUCTION

There is considerable research effort aimed at investigating and controlling molecular self-assembly. Indeed, this continues to be the principal approach employed in the development of novel nanotechnology. Typically the focus has been on functionalised molecules; however, such self-assembly also occurs in non-functionalised molecules such as saturated hydrocarbons. For example, when cooled from the molten state to ambient temperature, mixtures of normal paraffins (C_n:C_m) exhibit a wide range of solid state phase behaviour. For a certain carbon number (n-m), or equivalently chain-length mismatch, modulated structures form in the solid state. In the simplest case, an equimolar mixture of $C_{30}H_{62}$ and $C_{36}H_{74}$ (or $C_{36}D_{74}$) hydrocarbons will locally demix to form a modulated lamellar structure of alternating chains with a unit cell whose length corresponds to the sum of the long-spacings of the pure components [1]. We have made extensive studies on these materials and have shown that the repeat-spacing of the resultant structures may be controlled, not only by variation of the chain-length mismatch, but also molar composition, isotopic substitution, quench depth and confinement [2–5].

In our previous studies, and those of other workers, the alkane mixtures have typically been quenched rapidly from the melt to prevent macrophase separation. Here we report for the first time the effect of cooling protocol on normal alkane mixtures. We have prepared blends of $C_{28}H_{58}$ and $C_{36}D_{74}$ with a 2:1 molar ratio and studied them after subjection to a cooling rate that varied over three orders in magnitude with intermediate annealing prior to cooling to ambient. The protocol is observed to strongly impact upon the microstructure and indeed assists in greater ordering of the modulated demixed structure.

We have performed simultaneous small-angle X-ray scattering (SAXS) and differential scanning calorimetry (DSC) studies on the demixed systems as a function of cooling protocol. Their simultaneous collection enables the temperature-dependent nanostructural changes to be correlated with phase transitions. The data are further complemented by small-angle neutron scattering (SANS) highlighting

the separation of the individual chains via isotopic contrast and optical microscopy indicating changes occurring on the macroscopic scale.

EXPERIMENTAL

The pure paraffins were purchased from Aldrich ($C_{28}H_{58}$, 99%) and Cambridge Isotope Laboratories ($C_{36}D_{74}$, 98% at. D) and were used as received. A 2:1 molar composition mixture was prepared and placed in an oven for 15 minutes at 110°C, to allow the individual components to mix. After air-cooling, the samples were roughly ground and placed into modified DSC pans (see below). These samples were then remelted in the DSC at a rate of 100°C/min and cooled into the solid state following one of six cooling and annealing protocols (Fig. 1).

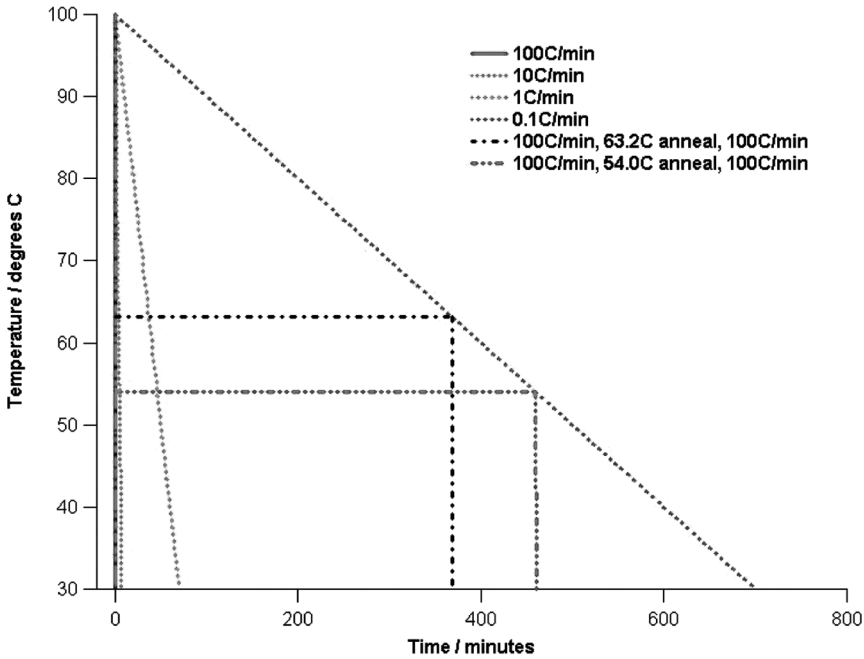

FIGURE 1 Schematic showing cooling protocols used in the experiments. Six protocols were used: cooling from 100°C to 30°C at i) 100°C/min, ii) 10°C/min, iii) 1°C/min and iv) 0.1°C/min. Two further samples were prepared using a double quench from 100°C to 63.2°C (mid-way between the onset of the first $C_{28}H_{58}$ transition and first $C_{36}D_{74}$ transition) and to 54.0°C (mid-way between the onset of the first $C_{28}H_{58}$ transition and onset of the mixing transition). Both samples were subsequently annealed and quenched to 30°C at 100°C/min.

These were cooling from 100°C to 30°C at 100°C/min (referred to as quenched), 10°C/min, 1°C/min and 0.1°C/min. Two further samples were prepared using a double quench from 100°C to: a) a temperature mid-way between the onset of the first $C_{28}H_{58}$ transition and first $C_{36}D_{74}$ transition, or b) a temperature mid-way between the onset of the first $C_{28}H_{58}$ transition and onset of the mixing transition. Both samples were subsequently annealed and quenched to 30°C at 100°C/min. These transition temperatures were selected based on initial DSC studies of the two pure components. The length of annealing time was determined as shown in Figure 1. All mixtures were aged for 3 weeks prior to study with SAXS and DSC (except for sample i which was studied after ca. 5 h). Optical micrographs of the samples were taken (*Zeiss Axioplan*) following the completion of the cooling procedure.

The SAXS measurements were performed on the new MPW6.2 station at the Synchrotron Radiation Source, Daresbury (United Kingdom) and represent the first SAXS user experiments from the new facility. The scattering vector, **q**, is defined as the difference between the incident and scattered X-ray or neutron wavevectors. For elastic scattering, $q = |\mathbf{q}| = (4\pi/\lambda)\sin\theta$, where 2θ is the angle through which the radiation is scattered and λ refers to the wavelength of the radiation used. The range of q accessed in the SAXS experiments was $0.009 \leq q/\text{Å}^{-1} \leq 0.276$ with $\lambda = 1.4\,\text{Å}$. The angular calibration of the quadrant SAXS detector was performed using an orientated specimen of wet rat-tail collagen. To minimise radiation damage to the sample a fast opening shutter was employed which was controlled by the acquisition computer. The shutter was programmed to open for the collection of the SAXS snapshots and was closed at all other times. SANS experiments were performed on the SAND instrument at the Intense Pulsed Neutron Source, Argonne National Laboratory (United States). Each sample, which had been enclosed in a 1 mm thick quartz cell, was placed in an oven at 100°C for 15 minutes prior to the cooling treatment.

The DSC measurements were performed on a *DSC600* system (Linkam Instruments, Surrey, England). The sample crucible possesses a slit of 4 mm by 1 mm making it suitable for X-ray transmission. The windows on the DSC experimental stage (which is designed for use with an optical microscope) were removed and fitted with mica windows for the SAXS measurements. The experimental stage was vertically mounted to allow transmission of the X-ray beam through the sample. Vertical orientation of the sample required the use of a spring of low thermal mass to hold the DSC pan against the heater plate. The DSC was calibrated with indium, tin, succinonitrile

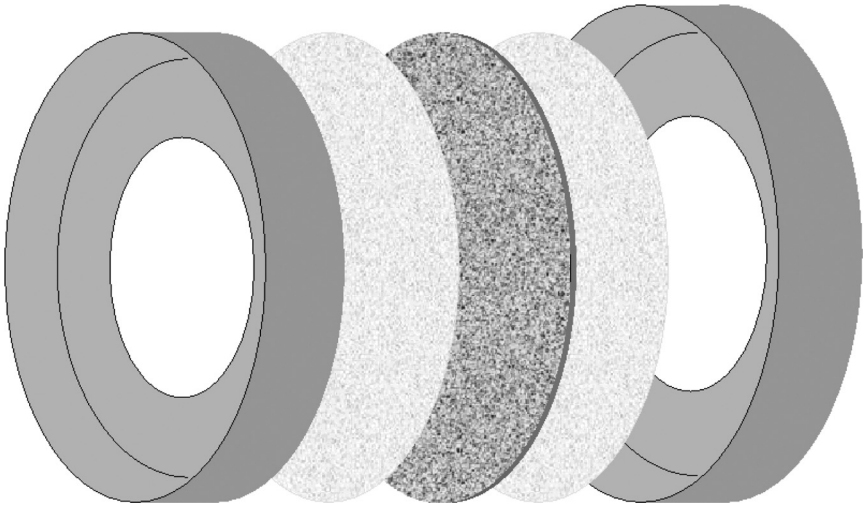

FIGURE 2 Schematic of modified DSC cell. The cell is composed of the aluminium pan and lid on the outside, followed by mica windows with the sample material in the centre.

and biphenyl. Modified aluminium DSC pans (*TA Instruments*) were used to hold the paraffin samples. Holes were punched in the base and lid of the pans. A disc of cleaved mica (of slightly smaller diameter than the pan base diameter) was placed in the base of the pan. The pan was then filled with the roughly ground paraffin mixture and another mica disc placed on top. After placing the lid on top the whole pan was crimped; this process ensures that the mica discs seal the windows punched in the pan (Fig. 2). The individual masses of the pan, mica windows and paraffin sample were recorded. Samples were heated and cooled with ramp rates of 1°C/min. The DSC and SAXS measurements were performed simultaneously, with 6 second snapshots of data taken every 30 seconds thus corresponding to data collection in 0.5 degree intervals.

RESULTS AND DISCUSSION

1. Pure Materials

The temperature-dependent SAXS and DSC from $C_{36}D_{74}$ and $C_{28}H_{58}$ are shown in Figure 3.

$C_{36}D_{74}$ exhibits three Bragg peaks, at 30°C, occurring at $0.133\,Å^{-1}$(47.2 Å); $0.149\,Å^{-1}$ (42.1 Å) and $0.161\,Å^{-1}$ (39.1 Å). These

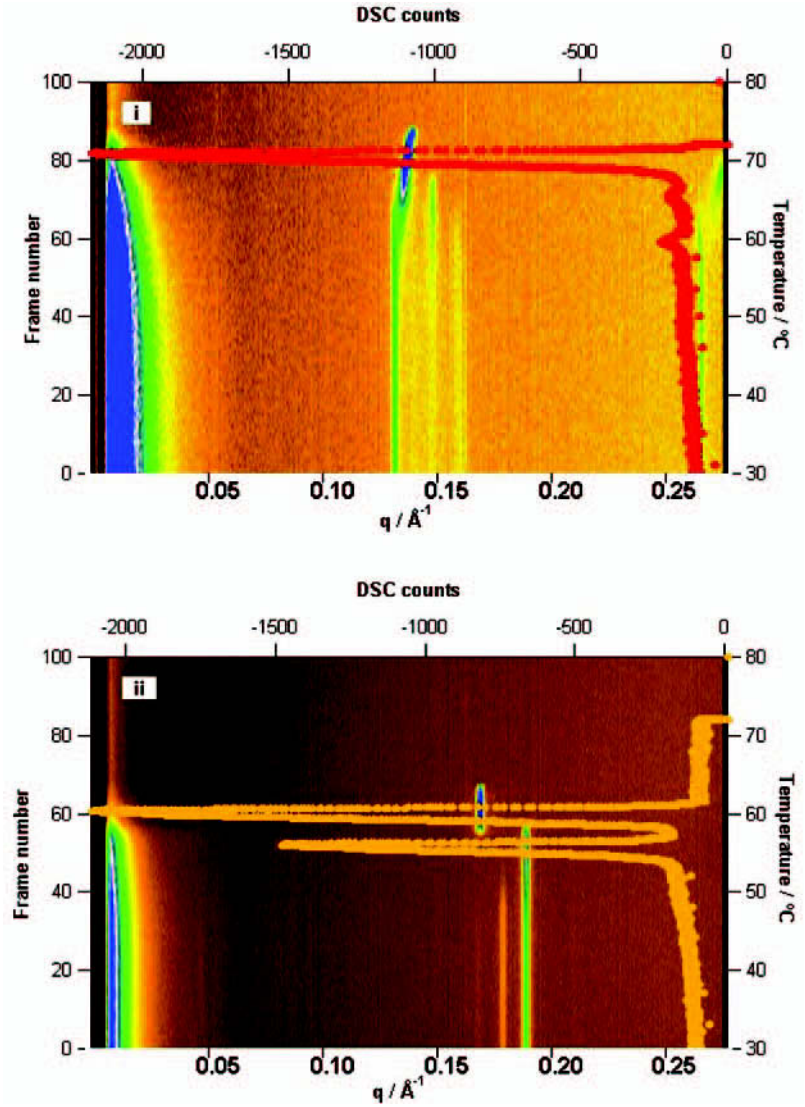

FIGURE 3 The temperature-dependent SAXS and DSC from i) $C_{36}D_{74}$ and ii) $C_{28}H_{58}$.

may be attributed to the orthorhombic (002 reflection) and two co-existing monoclinic (001) polymorphs of $C_{36}D_{74}$ respectively [6–8]. The monoclinic polymorphs exhibit a different temperature dependence with intensity transferring from the less stable, higher q, MII

to MI phase. There is a reduction in repeat spacing of the rotator phase as it approaches the melting transition that is associated with chain tilting from the orthorhombic form. The low angle scattering consistently decreases with temperature and is associated with surface scattering from crystalline domains. The orthorhombic and MII intensities disappear at approximately the same temperature, indicating a high degree of correlation, whereas the MI peak persists to higher temperatures via a rotator transition until melting. In the DSC, an intense melting endotherm is observed at 70.8°C. Two further endotherms occur at 59.5 and 65.1°C; these are extremely weak, however, and represent approximately 5% of the total enthalpy. The origin of these endotherms has not been investigated here although one is certainly likely to be associated with an orthorhombic to rotator transition.

$C_{28}H_{58}$ exhibits two low temperature peaks at $q = 0.180\,\text{Å}^{-1}$ (34.9 Å) and $0.190\,\text{Å}^{-1}$ (33.1 Å). These correspond to the triclinic and monoclinic (MI) 001 reflections. The triclinic phase is the less thermodynamically stable of the two low temperature polymorphs and this is evident from the transfer of intensity from the triclinic to monoclinic forms with increasing temperature. A monoclinic to rotator phase transition occurs at 56.0°C at $q = 0.170\,\text{Å}^{-1}$ (36.9 Å) with a corresponding reduction in low angle scattering. A rotator to melt transition occurs at 60.3°C. On cooling (not shown), no triclinic phase is present. In both pure materials, there is a significant correlation between the peak transition temperatures observed in the DSC with maxima in the Bragg peak intensity.

2. 2:1 $C_{28}H_{58}$:$C_{36}D_{74}$ Mixture

Figure 4 shows optical micrographs of six 2:1 $C_{28}H_{58}$:$C_{36}D_{74}$ mixtures differing only in their cooling protocol and its significant influence on their crystalline morphology. On the macroscopic scale, the crystalline domains increase in size and become less structured with decreasing cooling rate. Annealing at 54.0°C produces a more ordered morphology than 63.2°C. Simultaneous SAXS and DSC from the 100°C and 0.1°C/min samples and both double quenched samples are shown in Figure 5 over the full instrumental q range.

From a cursory inspection of the DSC plots, it is evident that the rapidly quenched sample gives rise to the most disordered structure; it exhibits an additional endotherm whose transition is close to the monoclinic to rotator transition observed for $C_{28}H_{58}$. The 63.2°C-annealed sample, while not exhibiting this additional endotherm, shows a strongly asymmetric lower temperature transition. The ratio of the lower to higher-temperature endotherm areas is approximately

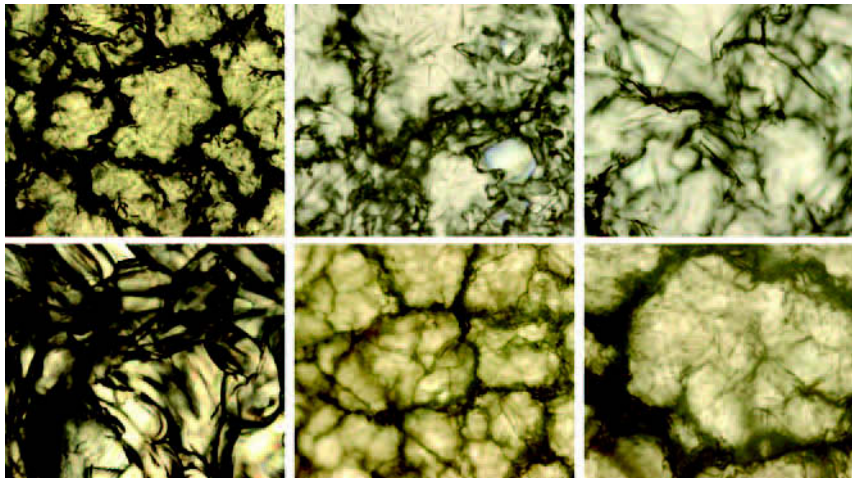

FIGURE 4 Optical micrographs from 2:1 $C_{28}H_{58}$:$C_{36}D_{74}$ mixtures showing influence of cooling protocol. The image size is 1.04 mm × 0.88 mm.

1:4 in these samples. The slow cooled and 54.0°C-annealed samples give rise to much sharper endotherms and the ratio of intensities are approximately 1:2.5. Based on previous SANS studies, we may certainly attribute the lower temperature endotherm to a mixing transition above which the demixed lamellar arrangement is destroyed [5]. Thus the greater ratio in the slow cooled and 54.0°C-annealed samples may be attributed to more extensive formation of the demixed structure. We also note that the mixing transitions occur approximately one degree higher in these samples. In related studies, the mixing transition has been shown to increase with aging time and is an indicator of the extent of formation of the demixed arrangement [9]. Similar intensity and positional trends are observed for the melting endotherm.

The melting transition for the mixture occurs close to the melting transition for pure $C_{28}H_{58}$ for all protocols. The transition temperature for the mixture is in reasonable agreement with the melting point depression predicted using Schröder's equation [10]. From the sum of the transition enthalpies from the solid to melt states for the paraffins and their corresponding melting points, we obtain a eutectic composition, x_E, of 0.8:0.2 $C_{28}H_{58}$:$C_{36}D_{74}$ and a eutectic temperature, T_E, of 60°C [2,11]. We note that the composition investigated here is hypereutectic relative to the predicted x_E and a separate $C_{36}D_{74}$ component is expected; however we observe no evidence for this in the SAXS.

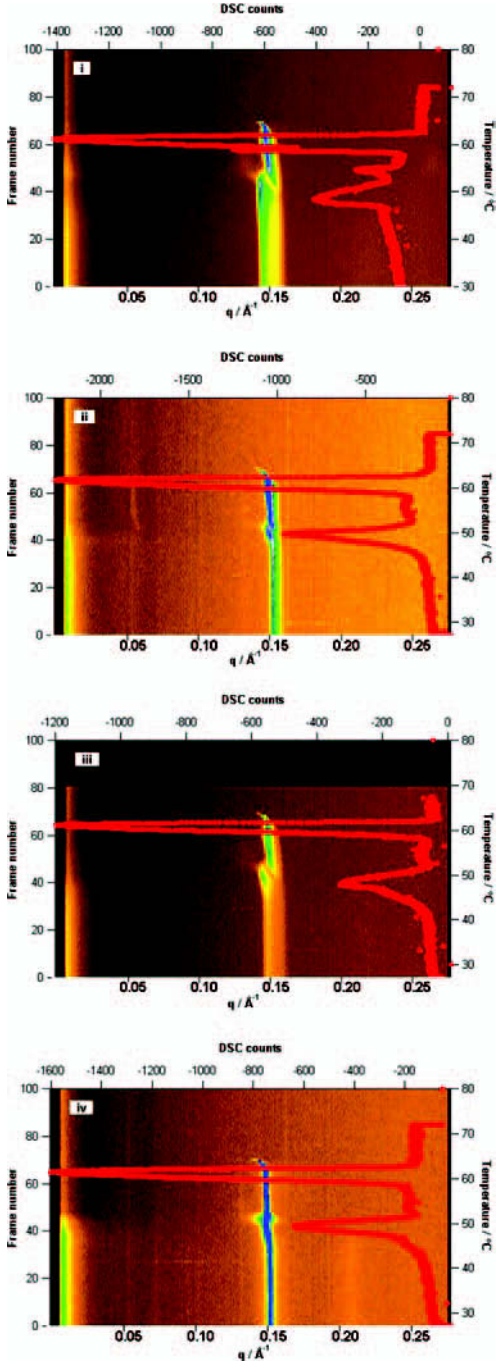

FIGURE 5 Temperature-dependent SAXS and DSC from i) 100°C/min (aged 5 h), ii) 0.1°C/min, iii) 63.2°C-annealed and iv) 54.0°C-annealed samples.

Scattering occurs almost exclusively from q = 0.12 to 0.18 Å$^{-1;}$ the data are plotted over this shorter range in Figure 6 to show more clearly the variation in peak shape and intensity with temperature. The samples exhibit a consistent ordering behaviour in the SAXS as in the DSC. For the rapidly cooled and higher-temperature annealed mixtures, a broad peak is observed at 30°C with a peak intensity corresponding to a 43.2 and 42.4 Å structure respectively. Conversely, the 54.0°C-annealed sample exhibits a single sharp peak at ca. 41 Å and the slow cooled sample a double peak with the lower angle feature also at ca. 41 Å. These numbers are in excellent agreement with Vegard's Law (molar average of orthorhombic unit cell lengths) again indicating that a more ordered structure has been formed [12]. The larger d-spacings observed in the former two samples indicate the formation of quenched-in voids. The higher q peak in the slow-cooled sample is associated with a distance of ca. 40 Å. It is not possible to unambiguously assign this peak to a second phase or a superstructure peak as the behaviour of the higher order reflections has not been probed over the experimental q range. For a separate phase, the

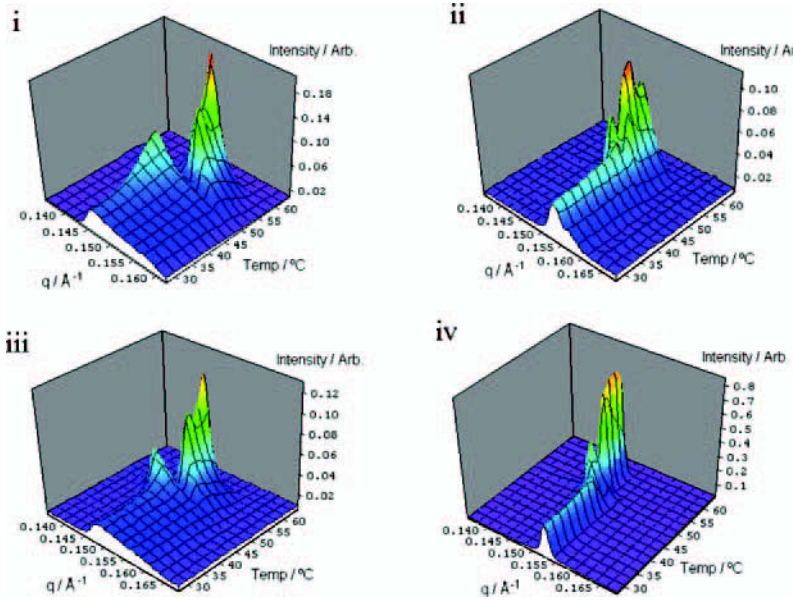

FIGURE 6 3D plots showing variation in SAXS for i) 100°C/min; ii) 0.1°C/min; iii) 63.2°C annealed and iv) 54.0°C annealed samples.

separation, Δq, between the peaks would increase with q; for a superstructure, Δq would be constant with q. This will be resolved in subsequent experiments.

While more extensive order is expected using a 0.1°C/min relative to 100°C/min cooling rate, a comparison of the two annealed samples indicates that maintaining the temperature a few degrees above the mixing transition greatly assists in the production of a more ordered modulated structure.

The variation in SAXS with increasing temperature is complex, yet a consistent picture emerges. Below the mixing transition, the Bragg peak associated with the demixed structure shifts to larger d-spacing and reaches its maximum intensity at approximately the peak transition temperature. This may be attributed to a gradual mixing of the chains and a disruption of the lamellar boundaries leading to an increase in the number of voids. SANS data show that the extent of demixing decreases, with decreasing quench depth, as the mixing transition is approached [3,5]. At the same temperature, a second higher q peak is apparent. Its intensity increases with temperature, while its position also increases with temperature until reaching a plateau below the melting transition. This lower d-spacing peak indicates an apparent shortening of one or both of the chains either via the formation of trans-gauche defects or a rotator phase. It is this chain modification that results in the destruction of the demixed phase.

The SAXS technique provides useful information on the 'average' lamellar chain structure but is far less sensitive to the modulated arrangement of chains. This is due to the minor difference in X-ray scattering length density between the components. The use of SANS, when one of the chains is isotopically labelled, enables the separation of protonated and deuterated chains to be easily determined. We have made preliminary, fixed-temperature, SANS measurements using the following cooling protocols: (i) quench to ambient (ca. 100°C min^{-1}), (ii) slow cool to ambient at 0.1°C min^{-1} and (iii) quench to 61°C, annealing for 11 h, followed by quenching to 25°C. The peak observed in the SANS is characteristic of the average separation of the protonated and deuterated chains [13] (Fig. 7). All samples show a characteristic spacing associated with a separation of approximately 120 Å. This is in excellent agreement with a hypothetical spacing based on a repeating arrangement of two $C_{28}H_{58}$ chains followed by a $C_{36}D_{74}$ chain in their characteristic orthorhombic packing arrangement (d = 123 Å) [6,8]. A comparison of the SANS data indicates more extensive formation of the demixed structure from both the scattering intensity and peak width in the slow cooled and low-temperature annealed samples. This not only supports the SAXS, DSC and microscopy data but also

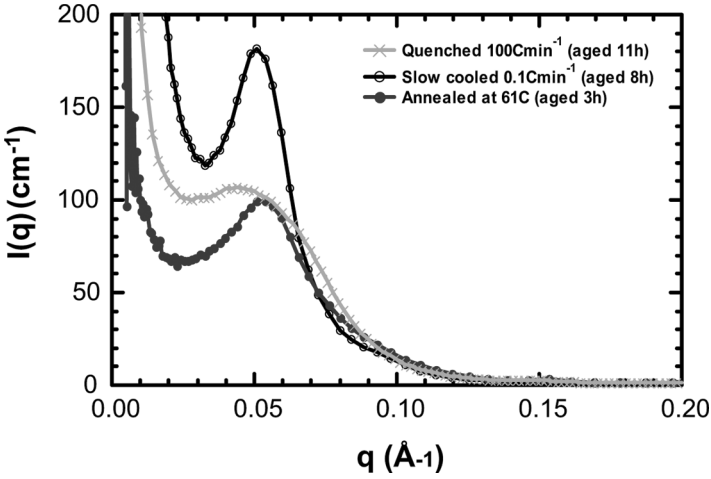

FIGURE 7 SANS from 2:1 $C_{28}H_{58}$:$C_{36}D_{74}$ mixtures highlighting effect of cooling protocol: quenched 100°C/min (crosses), slowly cooled at 0.1°C/min (open circles) and two-step quenching from 100°C to 61°C (annealed 11 h) and 61°C to 25°C (closed circles).

enables the dimension of the demixed structure to be deduced; this highlights the complementarity of neutron and X-radiation in these studies.

CONCLUSIONS

Time-resolved SAXS and DSC have been performed in parallel and correlated with optical microscopy and SANS. The data show that the cooling rate and annealing protocol are of fundamental importance to the demixed structure. Fast quenching (100°C/min) yields a similar arrangement to that obtained from annealing at temperatures between the melting points of the pure components. However, slow cooling (0.1°C/min) yields a far more ordered structure and gives is similar to that obtained from annealing at a temperature mid-way between the mixing transition and $C_{28}H_{58}$ melting point.

The results from these experiments will be correlated with further SANS studies, where the signal is monitored during temperature ramping, and where it is possible to benefit from the large scattering contrast between the protonated and deuterated components. We will also be conducting NMR and quasielastic neutron scattering, as a function of temperature to assist in our understanding of the extent of chain motion and its role on the observed transitions.

REFERENCES

[1] Gilbert, E. P., Reynolds, P. A., Brown, A. S., & White, J. W. (1996). n-Paraffin solid solutions: modification of phase separation with carbon number. *Chem. Phys. Lett.*, *255*, 373–377.

[2] Gilbert, E. P. (1999). The stability of binary C_n-C_{36} alkane mixtures. *Phys. Chem. Chem. Phys.*, *1*, 1517–1529.

[3] Gilbert, E. P., Reynolds, P. A., Thiyagarajan, T., Wozniak, D., & White, J. W. (1999). Kinetics of microphase separation in n-alkane mixtures. *Phys. Chem. Chem. Phys.*, *1*, 2715–2724.

[4] Gilbert, E. P. (1999). Incommensurate modulation of phase separating binary paraffin mixtures. *Phys. Chem. Chem. Phys.*, *1*, 5209–5214.

[5] Gilbert, E. P., Reynolds, P. A., & White, J. W. (1996). Microphase separation of binary paraffin mixtures adsorbed on graphite: Long time behaviour. *J. Phys. Chem.*, *100*, 18201–18213.

[6] Craig, S. R., Hastie, G. P., Roberts, K. J., & Sherwood, J. N. (1994). Investigation into the structures of some normal alkanes within the homologous series $C_{13}H_{28}$ to $C_{60}H_{122}$ using high-resolution synchrotron X-ray powder diffraction. *J. Mater. Chem.*, *4*, 977–981.

[7] Ohlberg, S. M. (1959). The stable crystal structures of pure *n*-paraffins containing an even number of carbon atoms in the range C_{30} to C_{36}. *J. Phys. Chem.*, *63*, 248–250.

[8] Nyburg, S. C. & Potworowski, J. A. (1973). Prediction of units cells and atomic coordinates for the *n*-alkanes. *Acta Cryst.*, *B29*, 347–352.

[9] Snyder, R. G., Conti, G., Strauss, H. L., & Dorset, D. L. (1993). Thermally-induced mixing in partially microphase segregated binary n-alkane crystals. *J. Phys. Chem.*, *97*, 7342–7350.

[10] Hsu, E. C. H. & Johnson, F. R. (1974). Prediction of eutectic temperatures, compositions and phase diagrams for binary mesophase systems. *Mol. Cryst. Liq. Cryst.*, *27*, 95–104.

[11] Gilbert, E. P. (1997). Phase Behaviour in n-Alkane Systems. PhD Thesis. Australian National University.

[12] Vegard, L. (1921). The constitution of mixed crystals and the space occupied by crystals. *Z. Physik.*, *5*, 17–26.

[13] White, J. W., Dorset, D. L., Epperson, J. E., & Snyder, R. (1990). Microphase separation in paraffin solid solutions. *Chem. Phys. Lett.*, *166*, 560–564.